JACS
JOURNAL OF THE AMERICAN CHEMICAL SOCIETY

Communication

pubs.acs.org/JACS

Controlled Co-Assembly of Nanoparticles and Polymer into Ultralong and Continuous One-Dimensional Nanochains

Phil Yong Kim, Jeong-Wook Oh, and Jwa-Min Nam*

Department of Chemistry, Seoul National University, Gwanak-ro 1, Gwanak-gu, Seoul 151-747, South Korea

Supporting Information

ABSTRACT: We report a robust one-dimensional (1D) nanoparticle-assembly strategy that uses the self-assembly of nanoparticles with ligand and thermal controls, polyethylene glycol (PEG) with thiol and carboxyl groups, and nanoparticle oligomer and polymer codewetting process to form ultralong and continuous 1D nanochains. The 1D nanochains were assembled with closely packed 1D nanoparticle oligomer building blocks, elongated and buttressed by dynamic 1D PEG templates formed on a hydrophobic surface via anisotropic spinodal dewetting. Using this strategy, nanoparticle-packed 1D nanochains (~1 nm interparticle spacing) were fabricated with ~60 nm-width and a few to >10 μm-length (nearly 20 μm in some cases) from 20 nm gold nanoparticles. Our findings offer insights and open revenues for particle assembly processes and, as given by 'universality in colloid aggregation', should be readily applicable to various nanoparticles.

The synthesis of diverse nanomaterials with distinct structural features and properties and tailoring the nanoarchitecture with accurate interparticle distance, specific packing, and directed orientation of nanoparticles (NPs) have been of paramount importance and challenge in materials science, chemistry, optics and nanotechnology. In particular, 1D assembly of NPs has drawn large attention for elucidating the formation mechanism of and building linear anisotropic constructs[1] and manufacturing a variety of nanodevices such as electrical devices,[1a,2b] plasmonic-magnetic nanocomposites,[1m] optical waveguides,[2a,c] and biochemical[1j,2d] and stress memory sensors.[2e] How the structural flexibility of 1D nanostructure[3b,d,e] affects (i.e., the arbitrary layouts of single-crystalline NPs and the end-fire excitations due to the local field enhancement at the junctions) and attenuates the scattering loss from structural defects[3a] or the bending loss in a continuous metal structure[3c] during light propagation has been of great interest.[2c,d,3] In addressing these issues and using the 1D nanostructures for practical applications, the pressing challenge is the assembly of the long, geometry-controlled and discrete 1D chains from NPs because it is difficult to control, align, and fix freely moving NPs in a specific direction and shape. Further, one should be able to comprehend and control the branching, bending, and close-packing behaviors of growing 1D nanostructures. Therefore, it would be beneficial if one can control the packing density and interparticle distance[3b,d] between NPs inside a 1D nanostructure and synthesize a targeted 1D structure with high structural precision and high yield. Although various NP assembly strategies have been developed using electron beam lithography-assisted 1D trench, polymer-mediated NP chain-growth, etc.,[1] it is still challenging to generate and control the geometry and detailed NP arrangement of 1D structures with nanometer precision.

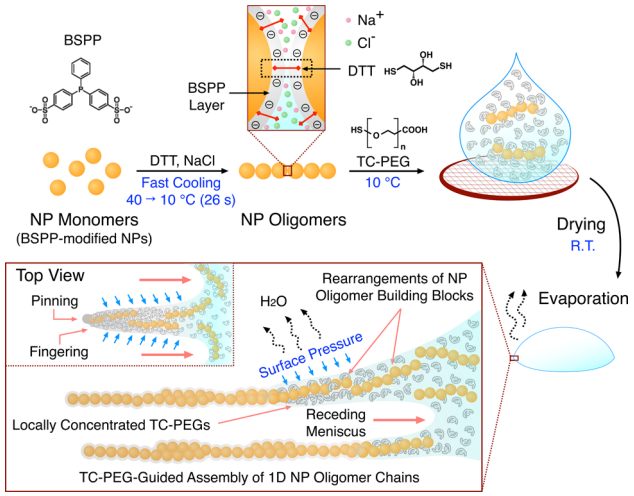

Figure 1. Schematic of controlled assembly of nanoparticle oligomer building blocks with heterobifunctional PEG (HS-PEG-COOH) into ultralong and continuous 1D nanochains.

Here we present a strategy to assemble NPs into ultralong and continuous 1D nanostructures through ligand control, thermal cooling-rate control, heterobifunctional PEG (HS-PEG-COOH; TC-PEG), and dewetting process. Using this strategy, without optimization of the dewetting process, we were able to assemble >10 μm-long and continuous NP chains with ~60 nm width and ~1 nm interparticle spacing. In our approach, we first formed relatively short 1D NP oligomers with bis(*p*-sulfonatophenyl)-phenylphosphine-modified Au NPs (BSPP-NPs) (Figures 1 and S1). These oligomers were formed via the end-on-type addition[1h] of NPs by quickly lowering temperature after the addition of NaCl and were further stabilized by dithiothreitol (DTT, ~1 nm length). These NP oligomers were then assembled, elongated, and buttressed by 1D TC-PEG templates formed on a hydrophobic surface via dewetting. Our subtle temperature control-based particle-assembly strategy could be applicable to various types of NPs because thermo-tunability is heavily dependent on the surface charges, not NP types.[4]

Received: May 11, 2015
Published: June 11, 2015

DOI: 10.1021/jacs.5b04714
J. Am. Chem. Soc. 2015, 137, 8030–8033

First, we optimized 1D NP oligomer formation process while controlling particle surface charge, cooling rate, and the temperature during particle assembly process. It was reported that the thermo-reversible assembly of NPs in a hydrogel system is possible by controlling temperature-dependent electrostatic repulsion,[5] and we reasoned that NPs could be directed into different self-assembly regimes via altering the reduction rate of electrostatic repulsion such as diffusion- vs rate-limited colloid aggregations.[1j,4] To test this hypothesis in an aqueous solution, we chose BSPP as the ligand (Table S1 and Figure S2) and set up the parameters that modulate the reduction rate of electrostatic repulsion. First, we lowered the temperature of BSPP-NP solution from 40 to 5 °C with 7 min 30 s cooling time and controlled the cooling rate by varying the holding time on the individual cooling steps, ranging from 1 to 5 min (see Supporting Information, SI). Figure S3a,b shows that BSPP-NPs fall into different self-assembly stages by changing the cooling rate. When the cooling rate was decreased, longitudinal plasmon couplings occurred more strongly with the formation of nanostructures at longer wavelengths (λ > 800 nm) by possibly forming nonlinear or branched nanostructures,[1e] and the isosbestic point of each assembly pathway was red-shifted from λ = 575 to 600 nm. When the solution was cooled more rapidly, the longitudinal plasmon coupling started appearing at λ = 700 nm, indicating the formation of 1D nanostructures (λ = 680−700 nm).[1j,3e]

After demonstrating that the 1D constructs were favorably formed by faster reduction in electrostatic repulsion, we tested the 1D structural evolution of BSPP-NPs by rapid cooling and tuning the final temperature of the colloidal solution. We lowered the temperature of the solution very quickly from 40 to a desired °C using a thermal cycler without intermediate holding steps, retained the final temperature for 1 min, and transferred the NP solution promptly to the cuvette at the given °C to monitor the particle self-assembly with an interval of 30 s (Figures 2a and S3c). A weak shoulder peak at λ = ∼680 nm was converted into a strong peak and plateaued within ∼5 min, while the peak at λ = ∼525 nm was dampened without a spectral shift. The trends were quite similar in each case except the 6 nm red-shift from the original peak (λ = 525 nm) at <8 °C. Notably, while lowering the final temperature, we observed that the difference in the peak intensities at λ = ∼525 (disassembled state) and ∼700 nm (assembled state) became smaller (the bottom plots of Figures 2a and S3c). From these observations, we selected the standard cooling rate, final temperature, and incubation time (i.e., 26 s from 40 to 10 °C, 7 min holding at 10 °C) in forming the 1D NP oligomers. In addition, the 1D oligomer generation process could be viewed as a rapid, thermo-reversible colorimetric detection platform (Figure S2).

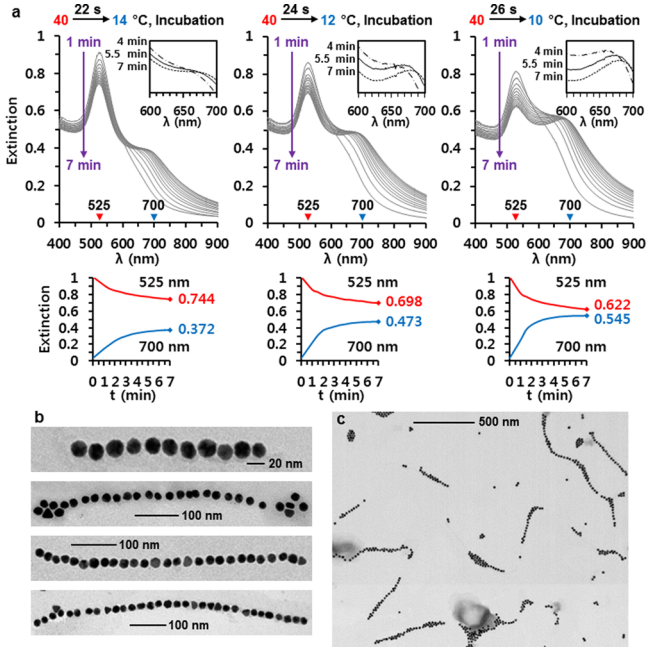

Figure 2. (a) Control in fast cooling to a specific temperature regulates the number of 1D chain-forming nanoparticles. Top right insets, the newly emerging peak at λ = ∼680 nm. (b) Fast cooling of BSPP-NPs, with NaCl, from 40 to 10 °C resulted in 1D nanoparticle oligomers. (c) 1D NP oligomers [the same condition applied as (b)].

We analyzed the assembled 1D NP oligomers with the transmission electron microscopy (TEM). Relatively short (230−650 nm) and linear nanochains were identified with the distinct nanogaps between NPs (Figure 2b). However, although some were straight and had a single-nanoparticle width, many of them were slightly curved and often stacked up with each other (Figures 2c and S4). Because they are temperature- and cation-sensitive, they can be broken and affected by change in temperature and local sodium ion concentration and evaporation-driven self-assembly while drying. As the size and shape of NPs were not completely uniform, this can induce two or more layered oligomer structures. To minimize the breaks in the 1D NP oligomers while drying and adding TC-PEG, DTT was added as an interparticle linker prior to the temperature control (Figure S1).

To direct the construction of highly stable, continuous, and long 1D nanochains, we introduced TC-PEG (3.4 or 5K) and employed this polymer as dynamic NP oligomer assembly templates. The thiol in TC-PEG acted as the "anchor" for the 1D NP oligomers to stably link Au NPs and the polymer, and the carboxyl group was also essential for the synthesis of 1D nanochains as discussed later. In both TC-PEG cases, we confirmed the formation of the nanowire-like TC-PEG thin film on a hydrophobic substrate via anisotropic spinodal dewetting[1f,6] including the fingering instability and the Saffman−Tayor instability[7] at room temperature (RT) after applying the same temperature control for the 1D oligomer synthesis to 2 μM TC-PEG solution (see the SI for mechanistic details). Upon evaporation, after the fingering instability[7c,e] and the coffee ring effect[8] influenced periodically TC-PEG-concentrated area at the air−water−substrate contact line, the critical aggregation concentration made the solvent pinning, which prevented the receding of water, and the thin films grew perpendicularly to the contact line. However, where the pinnings were absent, the evaporation-driven retraction of water made the growth of receding regions (or menisci). They could facilitate, cut off, and merge the growth of the thin film structures trapped between receding menisci (Figures 3a,b, S5, and S6). PEG can be crystallized into a helical structure by hydrophobic methylene groups via drying or heating.[9] The two different TC-PEG thin films formed micrometer-long nanowires (TC-PEG 5K: 7.4 ± 1.9 μm; TC-PEG 3.4K: 9.9 ± 3.6 μm; 10 longest nanochains were analyzed for each case) and were similar in width (TC-PEG 5K: 65 ± 15 nm; TC-PEG 3.4K: 67 ± 18 nm). This implies that the thin films of TC-PEG solution could be confined by unidirectional air flow. The evaporation at the receding meniscus front (the air−liquid interface) is basically the injection of the less viscous air-fluid into the dilute TC-PEG solution with larger viscosity and higher TC-PEG accumulation at the edge of

DOI: 10.1021/jacs.5b04714
J. Am. Chem. Soc. 2015, 137, 8030−8033

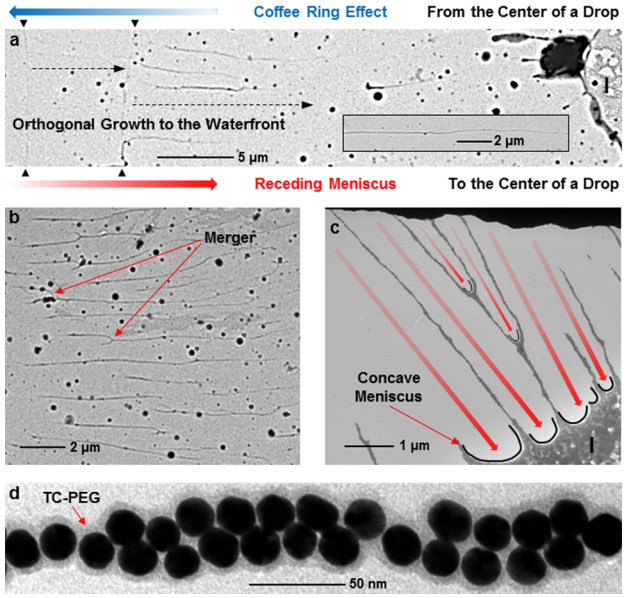

Figure 3. (a) Orthogonal growth of the thin films (TC-PEG 3.4K) to the local waterfront by receding menisci. Triangles, the water-substrate contact pinning line. I, the isotropic spinodal dewetting region. Inset, the nanowire-like TC-PEG thin films. (b) Nanowire-like TC-PEG 5K thin films. (c) Anisotropic dewetting process and concave menisci at the anisotropic–isotropic dewetting interface for the 1D nanoparticle chain assembly. (d) Magnified image of a 1D nanochain. NPs were clearly co-assembled and wrapped with TC-PEG.

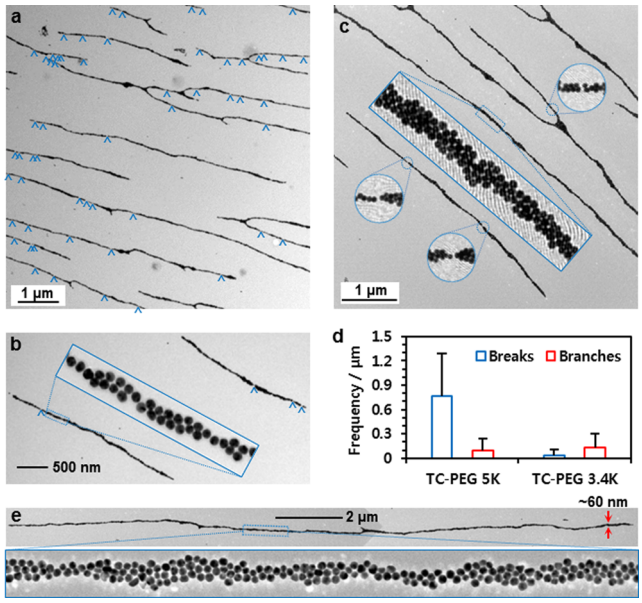

Figure 4. (a,b) Micrometer-long 1D chains with TC-PEG 5K. Inset in (b), the 1D chains had uniform thickness and were woven with the slanting single-line 1D nanoparticle oligomers. Brakets, >20 nm between two nearest nanoparticles. (c) TC-PEG 3.4K-based 1D chains. Insets, the magnified images as indicated. (d) Break and branching frequency in the 1D chains, mean ± SD. (e) Break-free, less-branched, and ultralong 1D chain with TC-PEG 3.4K template.

solution,[7f,8] and this is based on the Saffman–Taylor instability in which the invading air-finger width is the result of competition between the viscous (for reduction) and the capillary (for expansion) forces[7a] (or the inertia[7d] from a dilute polymer solution). At a given location, stable and wider fingers develop when polymer solution with less viscosity, and high surface tension is penetrated by the air fluid.[7a,b] Therefore, the thin TC-PEG film was narrowed down to nm-width and hardened over micrometer distances alongside the two air-fingers.

To synthesize ultralong 1D NP chains, in a typical experiment, the probe solution (BSPP-NPs, 1.2 nM) was supplemented with DTT (0.5 μM) at 40 °C for 30 min and was diluted to 0.5 nM with 10 mM sodium phosphate buffer, pH 7.4. Three tubes containing the probe (0.5 nM), NaCl (2 M), and TC-PEG (M_w = 3.4K or 5K; 3 μM, 75 mM NaCl), respectively, were put into a thermal cycler at 40 °C for 1 min, NaCl solution was quickly added to the probes (to 75 mM), and then incubating temperature was lowered to 10 °C after 26 s cooling. After 5 min incubation (incubation time was shortened because of DTT) at 10 °C, the probes without centrifugation were transferred to the TC-PEG solution, and 3 μL of the mixture was drop-cast and dewetted on a carbon-coated copper TEM grid at RT. As the drop evaporated, unlike spherical NPs that flourish at the edge of the drop, anisotropic structures (1D NP oligomers in our case) could be distributed more evenly in the form of open structures or chains at the air–water interface, which accounts for the uniform thickness in the final 1D nanochains, by the long-ranged, strong capillary attraction,[10] and TC-PEG prevented the NP oligomers from directly contacting with each other (the ratio of TC-PEG to BSPP-NP is 4000 to 1) until the thin film was formed. Without TC-PEG, the NP oligomers were heavily and uncontrollably aggregated because of DTT (Figure S7). Forming the NP oligomers with DTT and temperature controls as building blocks is, however, critical for the formation of very long 1D chains to avoid the incomplete and uncontrollable results (Figures S8 and S9). It is clear that the ultralong 1D nanochains can be synthesized by embedding of the NP oligomers within the 1D TC-PEG nanofilm as the thin film stiffens. As evaporation proceeded with the NP oligomers and TC-PEG, the air–water interface got closer to the substrate, and the thin films started to grow by forming inward propagating tips.[1f,7] The NP oligomers were trapped in the film-growing regions and were tilted and grew one dimensionally because the width of the thin TC-PEG film and the length of the oligomers are <100 nm and >100 nm, respectively. When the thin film developed and the distance between the oligomers shrank, the micrometer-long chains were packed linearly and held together by the thiols of TC-PEG and DTT on NPs. The role of the thiol of TC-PEG was confirmed by control experiment with PEG-COOH (Figure S10). The receding menisci[11] left the aligned array of μm-long 1D chains and the concave NP menisci at the anisotropic–isotropic dewetting interface (Figures 3c and S11). We also found the carboxyl group of TC-PEG is essential to form long and narrow nanochains (Figures S12 and S13).

Figure 4a,b shows a few to >10 μm-long nanochains with one or two nanoparticle-width, and nearly all the particles were one-dimensionally aligned with TC-PEG 5K. The chains were well separated, and, in some cases, branched structures were also found. It could be readily seen that the some parts of 1D chains were partially stacked and woven with the NP oligomer strips and that the linearity of the chains was maintained despite the bendable nature of these oligomers. This is because the assemblies of these 1D nanoparticle chains were guided by the nanowire-like TC-PEG templates that minimize the branching and bending of 1D structures. These 1D nanochains can be used for nanoantenna, waveguide, nanoplasmonics, and optoelectronics, and it is critical to have all the particles plasmonically coupled with each other throughout a chain for these

DOI: 10.1021/jacs.5b04714
J. Am. Chem. Soc. 2015, 137, 8030–8033

applications. Plasmonic coupling between two NPs becomes negligible when the interparticle gap is 2.5 times larger than the diameter of the NP.[12] Here, we counted the interparticle gap as a "break" when the gap size was >20 nm (we used 20 nm Au NPs). When TC-PEG 5K was used, several breaks were observed mainly at single-particle line portions (Figures 4a,b and S14). Significantly, with TC-PEG 3.4K, a majority of the nanochains did not have any break or had only one break over a whole nanochain (Figures 4c and S15). When >2 μm-long nanochains (24 chains) were analyzed for each TC-PEG case, 0.76 $\pm$ 0.53 and 0.035 $\pm$ 0.073 breaks per μm were found for TC-PEG 5K and 3.4K, respectively. The results suggest that lower-molecular-weight (MW) TC-PEGs induce higher orderliness[13b] and expose more thiols for the oligomer anchoring than the higher MW cases and, thus, develop an elevated tolerance[13c] in the 1D chains to the cracks[13a] typically found in dried samples. It should be also noted that 0.094 and 0.13 branches per μm were observed for TC-PEG 5K and 3.4K, respectively, mainly due to an unoptimized dewetting process (Figure 4d). Notably, >15 μm-long nanochains were often obtained with TC-PEG 3.4K (Figure 4e).

Our results offer insights and tools in self-assembly of NPs and precisely and readily assembling NPs into close-packed 1D nanochains with high controllability and high synthetic yield. We first formed NP oligomers by tuning the ligands, cooling rate, and temperature and then used the dewetting-based 1D TC-PEG thin film-forming process to organize the NP oligomers into ultralong and continuous 1D nanochains with ~1 nm interparticle spacing without any lithographic technique or predefined template. These findings could be useful for light manipulation, plasmonics, logical gate, optical sensors, optoelectronics, surface-enhanced Raman scattering, and on-chain lithography in conjunction with further improvements.[14]

■ ASSOCIATED CONTENT

Supporting Information

Experimental details and supplementary results. The Supporting Information is available free of charge on the ACS Publications website at DOI: 10.1021/jacs.5b04714.

■ AUTHOR INFORMATION

Corresponding Author

*jmnam@snu.ac.kr

Notes

The authors declare no competing financial interest.

■ ACKNOWLEDGMENTS

This work was supported by the National Research Foundation of Korea (2011-0018198) and the BioNano Health-Guard Research Center funded by the Ministry of Science, ICT & Future Planning of Korea as the Global Frontier Project (H-GUARD_2013M3A6B2078947).

■ REFERENCES

(1) (a) Lopes, W. A.; Jaeger, H. M. *Nature* **2001**, *414*, 735−738. (b) Warner, M. G.; Hutchison, J. E. *Nat. Mater.* **2003**, *2*, 272−277. (c) Jiang, K.; Eitan, A.; Schadler, L. S.; Ajayan, P. M.; Siegel, R. W.; Grobert, N.; Mayne, M.; Reyes-Reyes, M.; Terrones, H.; Terrones, M. *Nano Lett.* **2003**, *3*, 275−277. (d) Dujardin, E.; Peet, C.; Stubbs, G.; Culver, J. N.; Mann, S. *Nano Lett.* **2003**, *3*, 413−417. (e) Lin, S.; Li, M.; Dujardin, E.; Girard, C.; Mann, S. *Adv. Mater.* **2005**, *17*, 2553−2559. (f) Huang, J.; Kim, F.; Tao, A. R.; Connor, S.; Yang, P. *Nat. Mater.* **2005**, *4*, 896−900. (g) Kraus, T.; Malaquin, L.; Schmid, H.; Riess, W.; Spencer, N. D.; Wolf, H. *Nat. Nanotechnol.* **2007**, *2*, 570−576. (h) Zhang, H.; Wang, D. *Angew. Chem., Int. Ed.* **2008**, *47*, 3984−3987. (i) Chen, C.-L.; Rosi, N. L. *J. Am. Chem. Soc.* **2010**, *132*, 6902−6903. (j) Taylor, R. W.; Lee, T.-C.; Scherman, O. A.; Esteban, R.; Aizpurua, J.; Huang, F. M.; Baumberg, J. J.; Mahajan, S. *ACS Nano* **2011**, *5*, 3878−3887. (k) Shen, X.; Chen, L.; Li, D.; Zhu, L.; Wang, H.; Liu, C.; Wang, Y.; Xiong, Q.; Chen, H. *ACS Nano* **2011**, *5*, 8426−8433. (l) Wang, H.; Chen, L.; Shen, X.; Zhu, L.; He, J.; Chen, H. *Angew. Chem., Int. Ed.* **2012**, *51*, 8021−8025. (m) Adireddy, S.; Carbo, E. C.; Rostamzadeh, T.; Vargas, J. M.; Spinu, L.; Wiley, J. B. *Angew. Chem., Int. Ed.* **2014**, *53*, 4614−4617.

(2) (a) Maier, S. A.; Kik, P. G.; Atwater, H. A.; Meltzer, S.; Harel, E.; Koel, B. E.; Requicha, A. A. G. *Nat. Mater.* **2003**, *2*, 229−232. (b) Lee, D.; Choe, Y.-J.; Choi, Y. S.; Bhak, G.; Lee, J.; Paik, S. R. *Angew. Chem., Int. Ed.* **2011**, *50*, 1332−1337. (c) Solis, D.; Willingham, B.; Nauert, S. L.; Slaughter, L. S.; Olson, J.; Swanglap, P.; Paul, A.; Chang, W.-S.; Link, S. *Nano Lett.* **2012**, *12*, 1349−1353. (d) Cong, V. T.; Ganbold, E.-O.; Saha, J. K.; Jang, J.; Min, J.; Choo, J.; Kim, S.; Song, N. W.; Son, S. J.; Lee, S. B.; Joo, S.-W. *J. Am. Chem. Soc.* **2014**, *136*, 3833−3841. (e) Han, X.; Liu, Y.; Yin, Y. *Nano Lett.* **2014**, *14*, 2466−2470.

(3) (a) Ditlbacher, H.; Hohenau, A.; Wagner, D.; Kreibig, U.; Rogers, M.; Hofer, F.; Aussenegg, F. R.; Krenn, J. R. *Phys. Rev. Lett.* **2005**, *95*, 257403. (b) Lal, S.; Link, S.; Halas, N. J. *Nat. Photonics* **2007**, *1*, 641−648. (c) Wang, W.; Yang, Q.; Fan, F.; Xu, H.; Wang, Z. L. *Nano Lett.* **2011**, *11*, 1603−1608. (d) Halas, N. J.; Lal, S.; Chang, W.-S.; Link, S.; Nordlander, P. *Chem. Rev.* **2011**, *111*, 3913−3961. (e) Slaughter, L. S.; Willingham, B. A.; Chang, W.-S.; Chester, M. H.; Ogden, N.; Link, S. *Nano Lett.* **2012**, *12*, 3967−3972.

(4) Lin, M. Y.; Lindsay, H. M.; Weitz, D. A.; Ball, R. C.; Klein, R.; Meakin, P. *Nature* **1989**, *339*, 360−362.

(5) Liu, Y.; Han, X.; He, L.; Yin, Y. *Angew. Chem., Int. Ed.* **2012**, *51*, 6373−6377.

(6) (a) Higgins, A. M.; Jones, R. A. L. *Nature* **2000**, *404*, 476−478. (b) van Hameren, R.; Schön, P.; van Buul, A. M.; Hoogboom, J.; Lazarenko, S. V.; Gerritsen, J. W.; Engelkamp, H.; Christianen, P. C. M.; Heus, H. A.; Maan, J. C.; Rasing, T.; Speller, S.; Rowan, A. E.; Elemans, J. A. A. W.; Nolte, R. J. M. *Science* **2006**, *314*, 1433−1436.

(7) (a) Bensimon, D.; Kadanoff, L. P.; Liang, S.; Shraiman, B. I.; Tang, C. *Rev. Mod. Phys.* **1986**, *58*, 977. (b) Lindner, A.; Bonn, D.; Poiré, E. C.; Amer, M. B.; Meunier, J. *J. Fluid Mech.* **2002**, *469*, 237−256. (c) Lyushnin, A. V.; Golovin, A. A.; Pismen, L. M. *Phys. Rev. E* **2002**, *65*, 021602. (d) Chevalier, C.; Amar, M. B.; Bonn, D.; Lindner, A. *J. Fluid Mech.* **2006**, *552*, 83−97. (e) Craster, R. V.; Matar, O. K. *Rev. Mod. Phys.* **2009**, *81*, 1131. (f) Agam, O. *Phys. Rev. E* **2009**, *79*, 021603.

(8) Deegan, R. D.; Bakajin, O.; Dupont, T. F.; Huber, G.; Nagel, S. R.; Witten, T. A. *Nature* **1997**, *389*, 827−829.

(9) (a) French, A. C.; Thompson, A. L.; Davis, B. G. *Angew. Chem., Int. Ed.* **2009**, *48*, 1248−1252. (b) Asada, M.; Jiang, N.; Sendogdular, L.; Sokolov, J.; Endoh, M. K.; Koga, T.; Fukuto, M.; Yang, L.; Akgun, B.; Dimitrioug, M.; Satijag, S. *Soft Matter* **2014**, *10*, 6392−6403.

(10) Yunker, P. J.; Still, T.; Lohr, M. A.; Yodh, A. G. *Nature* **2011**, *476*, 308−311.

(11) Bensimon, A.; Simon, A.; Chiffaudel, A.; Croquette, V.; Heslot, F.; Bensimon, D. *Science* **1994**, *265*, 2096−2098.

(12) Su, K.-H.; Wei, Q.-H.; Zhang, X.; Mock, J. J.; Smith, D. R.; Schultz, S. *Nano Lett.* **2003**, *3*, 1087−1090.

(13) (a) Lee, W. P.; Routh, A. F. *Langmuir* **2004**, *20*, 9885−9888. (b) Kline, R. J.; McGehee, M. D.; Kadnikova, E. N.; Liu, J.; Fréchet, J. M. J; Toney, M. F. *Macromolecules* **2005**, *38*, 3312−3319. (c) Prosser, J. H.; Brugarolas, T.; Lee, S.; Nolte, A. J.; Lee, D. *Nano Lett.* **2012**, *12*, 5287−5291.

(14) (a) Huo, F.; Zheng, Z.; Zheng, G.; Giam, L. R.; Zhang, H.; Mirkin, C. A. *Science* **2008**, *321*, 1658−1660. (b) Wang, F.; Liu, X. *Chem. Soc. Rev.* **2009**, *38*, 976−989. (c) Chen, G.; Wang, Y.; Yang, M.; Xu, J.; Goh, S. J.; Pan, M.; Chen, H. *J. Am. Chem. Soc.* **2010**, *132*, 3644−3645. (d) Wei, H.; Wang, Z.; Tian, X.; Käll, M.; Xu, H. *Nat. Commun.* **2011**, *2*, 387. (e) Sheldon, M. T.; van de Groep, J.; Brown, A. M.; Polman, A.; Atwater, H. A. *Science* **2014**, *346*, 828−831.

DOI: 10.1021/jacs.5b04714
J. Am. Chem. Soc. 2015, 137, 8030−8033